Oscillatory magnetotransport in $NbSe_3$ and $TaSe_3$†*

R. M. Fleming, J. A. Polo, Jr., and R. V. Coleman
Department of Physics, University of Virginia, Charlottesville, Virginia 22901
(Received 5 August 1977)

Shubnikov–de Haas oscillations in $NbSe_3$ and $TaSe_3$ have been observed in the field range 0–170 kG using both ac and dc techniques. The Fermi-surface sections have been tracked over a substantial angular range and the observed anisotropies are consistent with elongated ellipsoids. In $NbSe_3$ a single section with a minimum frequency of 0.28 MG dominates the oscillatory behavior and develops a strong harmonic content at high fields. Fits of the data to expressions including the spin splitting of the Landau levels gives a minimum g factor of 3.2 and a Dingle temperature of $T_D = 2.3$ K. The temperature dependence of the amplitude gives an effective mass of 0.24 for this section. The Hall effect has also been measured in $NbSe_3$ and shows a sign change from positive to negative as the temperature is decreased below the 59-K transition in $NbSe_3$. No significant change is observed near the 145-K transition. In $TaSe_3$ at least 20 frequencies in the range 0.7–22 MG have been observed and these exhibit a distribution of fairly strong amplitudes with no single frequency dominating. The crystals of $NbSe_3$ and $TaSe_3$ are of comparable quality and resistance ratio so the results indicate that the Fermi surfaces have quite different parameters in the two metals.

I. INTRODUCTION

The transition-metal trichalcogenides $NbSe_3$ and $TaSe_3$ are highly anisotropic metals with each metal atom at the center of a trigonal prism of selenium atoms which are arranged in chains along the $\hat{b}$ axis. Although the crystal structures are similar the transport properties show significant differences which imply major differences in the band structure and Fermi surfaces of these two metals. $NbSe_3$ shows two major anomalies in the resistivity versus temperature which occur at 145 and 59 K as shown in Fig. 1(a). Such anomalies are not observed in $TaSe_3$ as shown in the resistivity data of Figs. 1(b) and 2(a). Below 145 K $NbSe_3$ exhibits nonohmic behavior clearly associated with the transitions and studied in detail by Monceau *et al.*[1] and by Ong and Monceau.[2] Such resistive transitions suggest the possibility that charge-density-wave (CDW) transitions are occurring similar to those observed in the layer-structure dichalcogenides.[3] The formation of a CDW in $NbSe_3$ would substantially modify the Fermi surface and could account for the large difference in electronic behavior observed in $NbSe_3$ vs $TaSe_3$ although considerably more work including x-ray and neutron-diffraction experiments will be needed to establish CDW formation in $NbSe_3$. In this paper we report magnetotransport measurements on both $NbSe_3$ and $TaSe_3$ and use the quantum oscillations observed in the magnetoresistance to obtain information on the Fermi surfaces of the two materials.

Both $NbSe_3$ and $TaSe_3$ grow as long thin fibrous ribbons or needles composed of trigonal prisms stacked along the fiber axis which is parallel to the $\hat{b}$ axis as shown in Fig. 3(a). Each chain of prisms is displaced relative to its neighbor so that

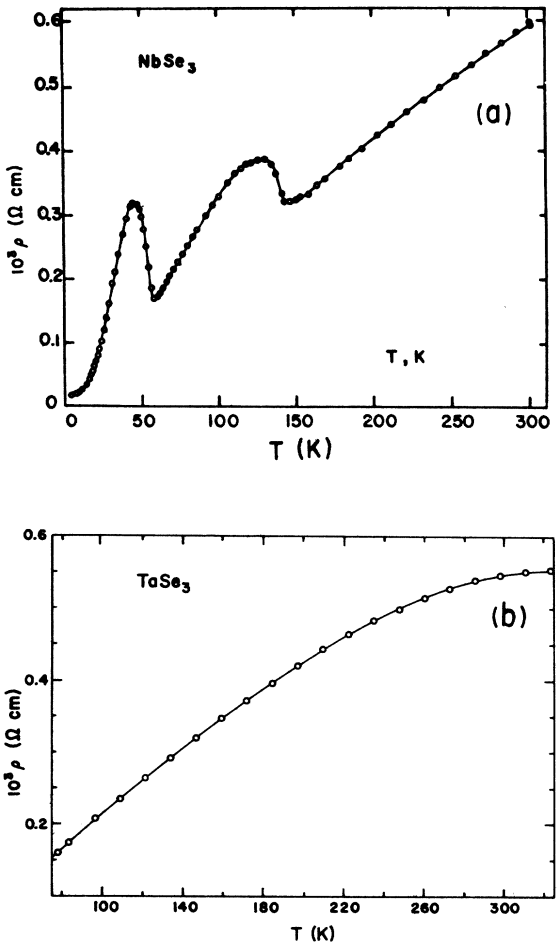

FIG. 1. (a) Temperature dependence of resistivity in $NbSe_3$ showing the two resistive transitions at 145 and 59 K, respectively. (From Ref. 2.) (b) Temperature dependence of resistivity in $TaSe_3$ in the range 77–323 K.

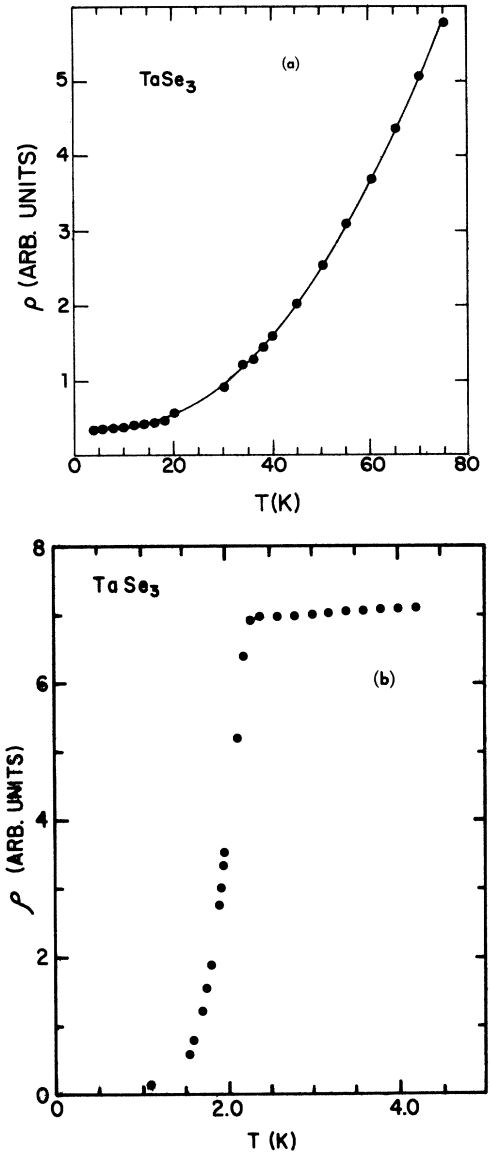

FIG. 2. (a) Temperature dependence of resistivity of $TaSe_3$ in the range 4.2–80 K; (b) temperature dependence of resistivity of $TaSe_3$ in the range 1.1–4.2 K showing superconducting transition at ~ 2 K.

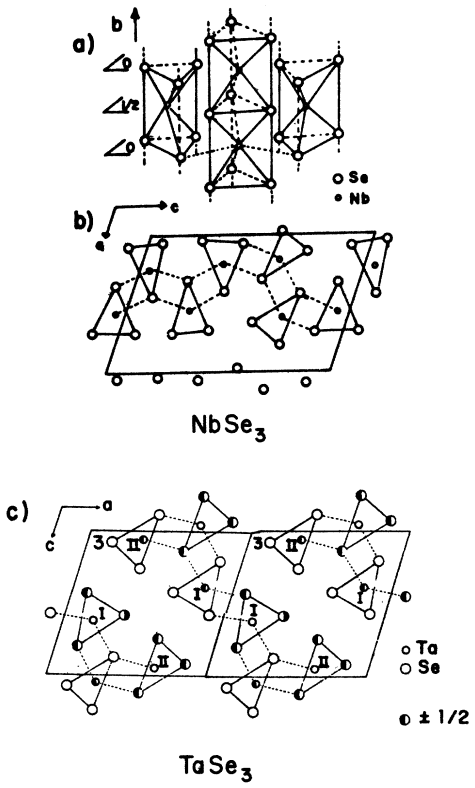

FIG. 3. Atomic arrangements for the $NbSe_3$ and $TaSe_3$ structures (a) stacking of prisms along the $\hat{b}$ axis; (b) projection of the $NbSe_3$ structure in the $\hat{a}$-$\hat{c}$ plane; and (c) projection of the $TaSe_3$ structure in the $\hat{a}$-$\hat{c}$ plane.

all atoms lie along planes separated by $\frac{1}{2}\hat{b}$. The arrangement of atoms in these planes is shown in Figs. 3(b) and 3(c). X-ray work shows the crystal structure to be monoclinic for both materials.[4,5] In the case of $NbSe_3$ six chains are contained in the unit cell with the prisms arranged as shown in Fig. 3(b), while in $TaSe_3$ there are four chains per unit cell with the prisms in a slightly different arrangement, as shown in Fig. 3(c). The distance between metal atoms along the chains is much closer (3.478 for $NbSe_3$ and 3.495 for $TaSe_3$) than the interprism metal-atom distances which give distances between metal atoms in the range 4–4.3 Å. In addition, there is substantial anisotropy in the metal-atom spacing in the $\hat{a}$-$\hat{c}$ plane, as shown in Fig. 3. These anisotropies can be expected to produce large angular variations in the transport properties. The highest conductivity would be expected along the $\hat{b}$ axis although the present measurements indicate that the Fermi surface remains three dimensional in both materials.

In addition to the differences in normal metal transport properties the occurrence of superconductivity is significantly different in the two cases. At atmospheric pressure $NbSe_3$ does not show a superconducting transition, while at increased pressures it becomes superconducting with T_c rising to ~2.5 K at 7 kbar as reported by Monceau *et al.*[6] In the case of $TaSe_3$ at atmospheric pressure, we find a T_c of ~2 K as shown in Fig. 2(b). However, Monceau *et al.*[6] report that $TaSe_3$ is not superconducting at any pressure up to 6.5 kbar. Sambongi *et al.*[7] have recently reported that $TaSe_3$ is superconducting with a T_c of 2.1 K in substantial agreement with our measurements. These results suggest that the interplay between the electron-

phonon interaction, the electronic structure, and superconductivity, is carefully balanced in both of these materials and that perturbations can alter the superconductivity very rapidly.

II. EXPERIMENTAL TECHNIQUES

The magnetotransport measurements have been made in field ranges up to 170 kG. A superconducting solenoid has been used for the range up to 70 kG and bitter solenoids at the National Magnet Laboratory and at the Naval Research Laboratory have been used for the higher-field ranges. The magnetoresistance has been measured using both a standard dc technique with a high-sensitivity dc voltage measurement and an ac field-modulation technique with second harmonic detection.[8] In the case of the superconducting solenoid a separate superconducting modulation coil with a maximum field of ~500 G was installed on the tail of the inner helium Dewar. For ac measurements on the Bitter solenoids the generator current was modulated giving a maximum modulation field of approximately 5 kG peak to peak at 7.5 Hz.

For both ac and dc measurements the curves were recorded simultaneously on an x-y recorder and on paper tape. The frequencies of the quantum oscillations were then analyzed by computer using a fast Fourier transform program. Typically 700 points were recorded per field sweep giving a frequency resolution in the transform of 0.06 MG or better. Both the ac and dc measurements were in agreement at the low-frequency end of the spectrum, while the higher frequencies and lower-amplitude frequencies were well resolved only with the high-sensitivity ac method. Most of the measurements were made in a pumped bath of liquid helium at a temperature of ~1.1 K. In a few cases the effective mass has been determined by measuring the temperature dependence of the amplitude in the range 4.2–1.1 K.

The crystals were grown by direct sublimation of the elements in evacuated quartz tubes. The growth chamber was heated to ~700 °C and maintained with a temperature gradient of 40 °C for a period of two weeks. The whiskerlike strands of crystal grow up to approximately 5 cm in length and are oriented along the $\hat{b}$ axis. The cross sections of $NbSe_3$ were approximately 0.2 mm × 0.005 mm and the cross sections for $TaSe_3$ were 0.2 mm × 0.1 mm. The residual resistance ratios $R_{300\,K}/R_{4.2\,K}$ were on the order of 200 for $NbSe_3$ and on the order of 80 for $TaSe_3$.

The leads for resistance or Hall measurements were attached to the $NbSe_3$ crystals with silver paint, while the $TaSe_3$ leads were soldered to sputtered copper contacts. Most of the samples for oscillatory measurements were mounted on circuit boards in rotating sample holders immersed directly in the liquid-helium bath. The temperature dependence of resistance, magnetoresistance, and Hall effect were made using variable-temperature sample holders operated with resistance heaters and helium exchange gas. The temperature was controlled and measured using both resistance and capacitance thermometers. The temperature control in high magnetic fields was generally done with capacitance sensors due to their field-independent behavior.

III. EXPERIMENTAL RESULTS

A. Magnetoresistance in $NbSe_3$

Both dc and ac magnetoresistance curves in the range 0–170 kG have been recorded for $NbSe_3$. For the ribbon-shaped crystals transverse magnetoresistance curves have been obtained for a range of field directions lying in the plane perpendicular to the $\hat{b}$ axis. For transverse fields parallel to the plane of the ribbon the dc magnetoresistance curve is dominated by a single large-amplitude quantum oscillation of frequency 0.28 MG as shown in Fig. 4. At high fields the magnetoresistance peaks are split due to the presence of the second harmonic. The transverse-rotation diagrams show minima for field directions parallel to the plane of the ribbon and maxima for fields perpendicular to the plane of the ribbon. The background dc magnetoresistance shows an essentially linear field dependence for all transverse-field directions.

The angular dependence of the quantum oscillations for intermediate-field angles between parallel and perpendicular to the plane of the ribbon has been measured with both dc and ac techniques. The Fourier-transform results from both types of measurement give essentially consistent frequencies although the ac method gives greater accuracy. The angular dependence of the frequencies in the

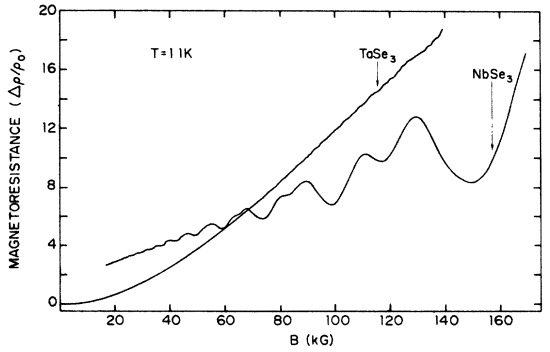

FIG. 4. Transverse magnetoresistance of $NbSe_3$ and $TaSe_3$ for current along the $\hat{b}$ axis. $\vec{B} \| \hat{c}$ in the plane of the ribbon for $NbSe_3$.

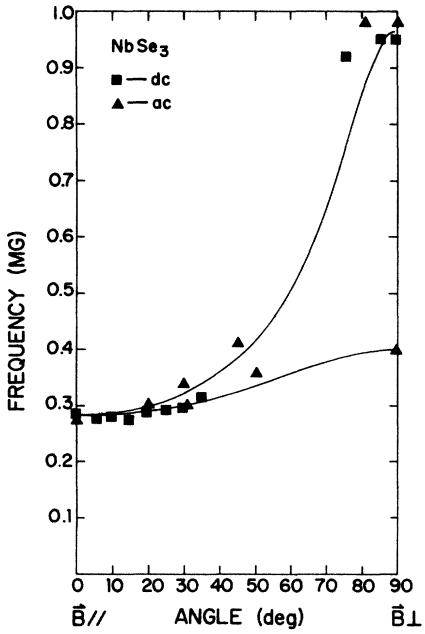

FIG. 5. Angular dependence of the lowest frequency branches in $NbSe_3$ observed for field directions lying in the $\hat{a}$-$\hat{c}$ plane. $\hat{c}$ axis is the plane of the ribbon $\perp$ to $\hat{b}$.

plane perpendicular to the $\hat{b}$ axis is shown in Fig. 5. Very strong amplitudes are observed in the angular range from 0 to 50° and near 90° (perpendicular to plane of ribbon). In the range 50°–70° off the plane of the ribbon the amplitudes are weak and precise frequencies have not been determined. There seem to be at least two frequency branches in the above angular range although the data do not precisely separate them except at 90°. The solid lines drawn in Fig. 5 represent the frequency branches expected for ellipsoids of revolution with anisotropy ratios of 3.4 and 1.4, respectively.

The angular dependence of the frequencies corresponding to field directions rotated toward $\hat{b}$ and lying in the plane of the ribbon is shown in Fig. 6. In this case the low frequency with a value of 0.28 MG for $\vec{B} \perp \hat{b}$ dominates over most of the angular range. Both the second and third harmonic of this frequency track over most of the angular range and the harmonics are also plotted in Fig. 6. The solid lines represent functions of the form $\omega_0/(\epsilon^2 \sin^2\theta + \cos^2\theta)^{1/2}$ with $\epsilon = \frac{1}{8}$. These functions represent the angular variation of the cross sections of ellipsoids with an anisotropy of 8 (ratio of major to minor axis is 8). This represents an approximate lower limit on the anisotropy since the data cannot distinguish between anisotropies of 8 or greater. The upper dashed line corresponds to $\epsilon = 0$ and the lower dashed line to $\epsilon = \frac{1}{5}$.

At field angles between 20° and 60° off the $\hat{a}$-$\hat{c}$ plane, we definitely detect Fourier components

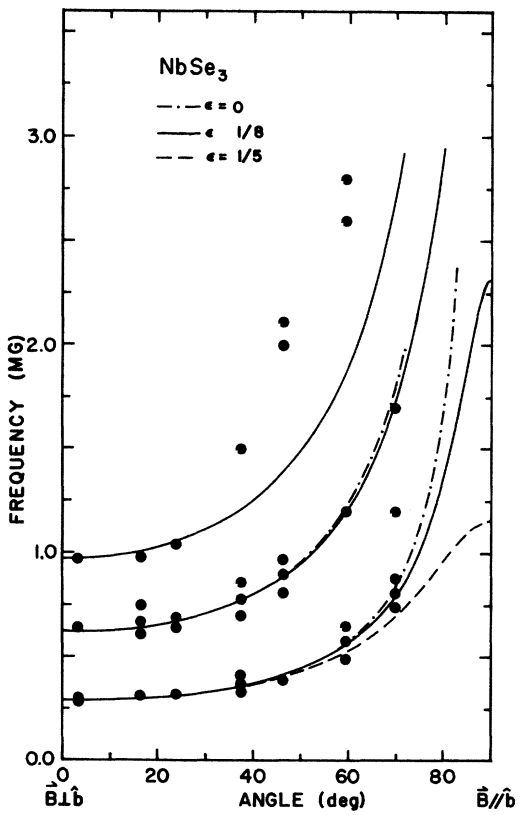

FIG. 6. Angular dependence of the lowest frequency branch in $NbSe_3$ and its second and third harmonics observed for field directions rotated from the $\hat{a}$-$\hat{c}$ plane toward $\hat{b}$. Plots start at the field direction parallel to the ribbon corresponding to the minimum frequency in the $\hat{a}$-$\hat{c}$ plane. Solid lines represent a function of the form $\omega_0/(\epsilon^2 \sin^2\theta + \cos^2\theta)^{1/2}$ with $\epsilon = \frac{1}{8}$. Dashed lines show this function with $\epsilon = 0$ and $\epsilon = \frac{1}{5}$. A few higher frequencies not associated with the lowest branch are also shown.

at higher frequencies in the range 1–3 MG. Points corresponding to the strongest of these additional frequencies are also plotted in Fig. 6, however, the data on the higher frequencies are insufficient to identify an additional branch over the entire angular range.

The ac magnetoresistance plots for the parallel- and perpendicular-field orientations show the greatest amplitudes and typical examples are shown in Fig. 7. The Fourier transforms for these curves are shown in Fig. 8 and show very strong peaks corresponding to the frequencies plotted in Figs. 5 and 6. In addition, peaks corresponding to harmonics of these strong frequencies are seen as well as some weaker peaks at higher frequencies. This suggests that the present experiments may not be detecting larger sections of the Fermi surface although the oscillatory transport is certainly dominated by two very strong low frequencies.

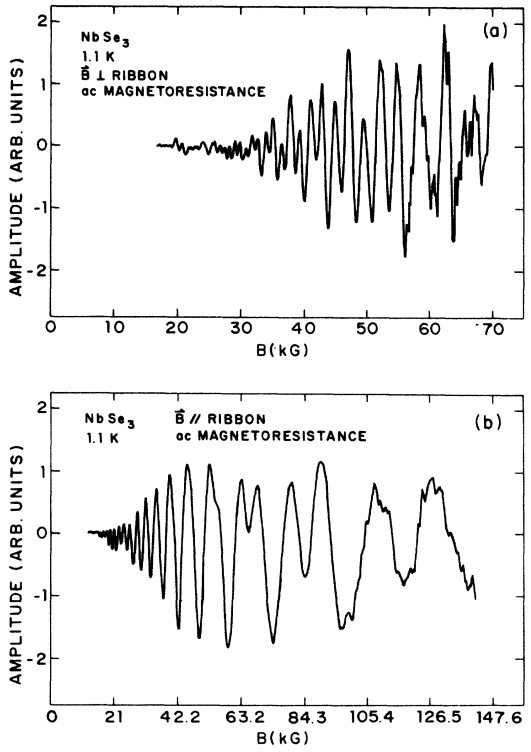

FIG. 7. Representative ac magnetoresistance curves measured for $NbSe_3$: (a) 15–70 kG; (b) 15–142 kG.

B. Magnetoresistance in $TaSe_3$

Both dc and ac magnetoresistance curves have also been recorded for $TaSe_3$. The transverse dc magnetoresistance shows only small-amplitude oscillations in the highest-field range, as shown

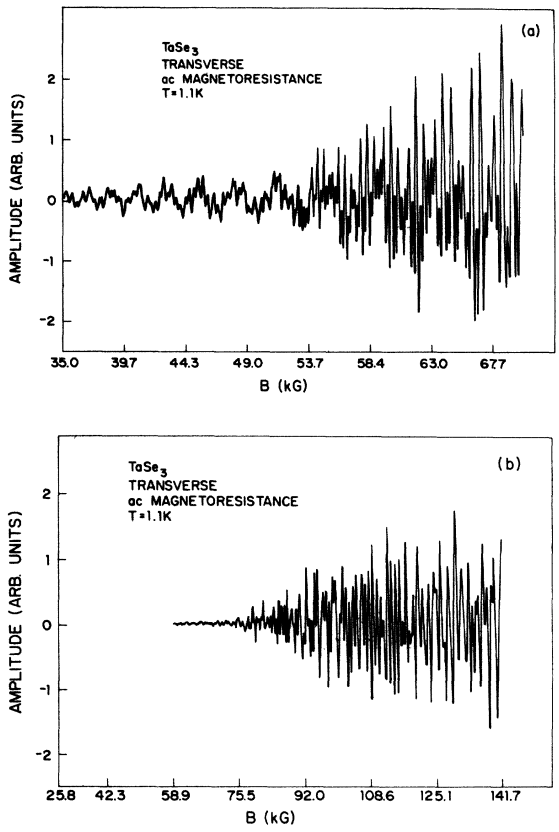

FIG. 9. Representative ac magnetoresistance curves measured for $TaSe_3$ with magnetic field transverse to the $\hat{b}$ axis. (a) 35–70 kG field in $\hat{a}$-$\hat{c}$ plane at the minimum frequency direction; (b) 37–142 kG field in $\hat{a}$-$\hat{c}$ plane 14° off minimum frequency direction.

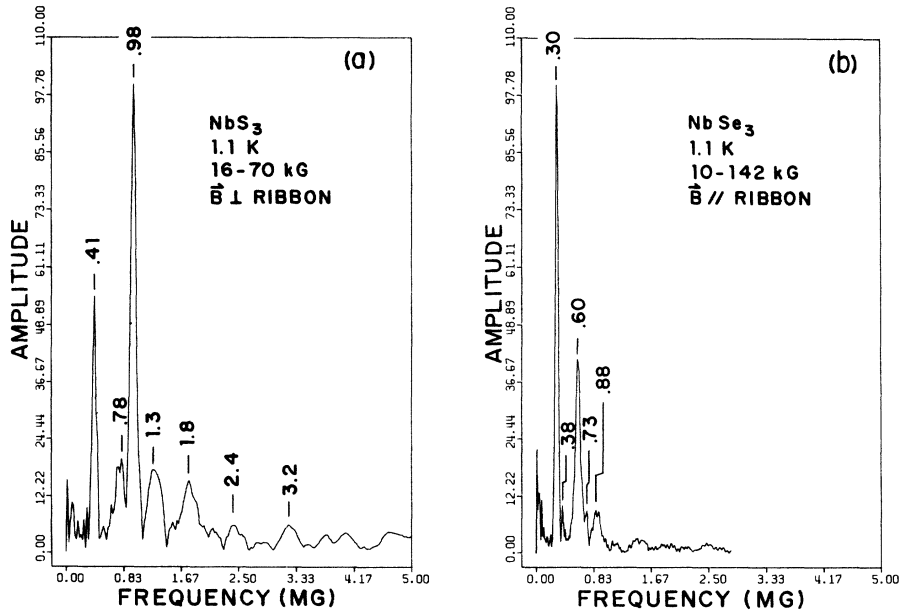

FIG. 8. Fourier transforms of the ac magnetoresistance plots shown in Fig. 7. (a) For $\vec{B}$ perpendicular to the ribbon two strong frequency branches are observed plus additional weak frequencies; (b) for $\vec{B}$ parallel to the ribbon the fundamental and two harmonics dominate the spectrum.

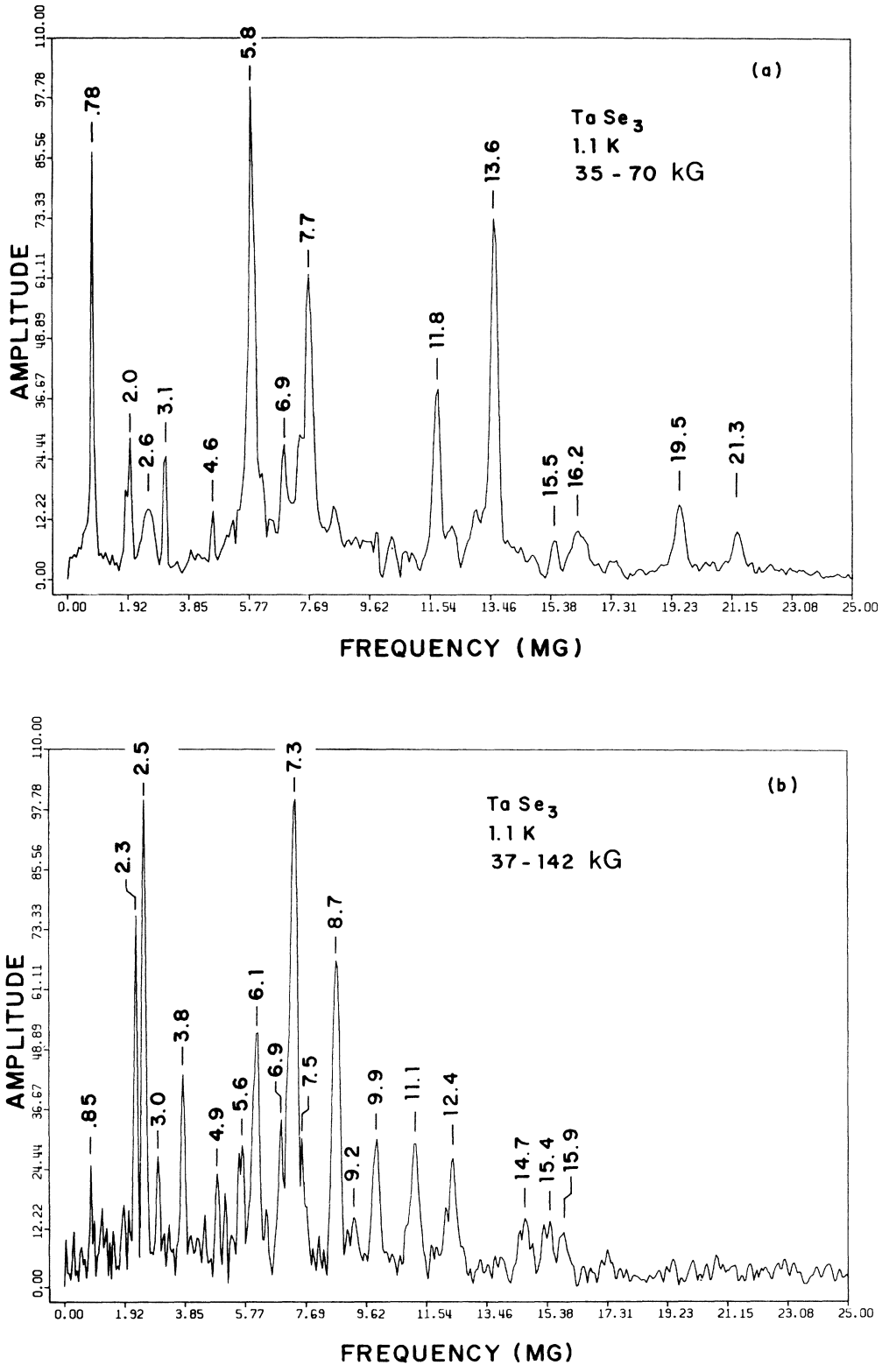

FIG. 10. Fourier transforms of the ac magnetoresistance data shown in Fig. 9. (a) At least 14 frequencies are resolved in this transform. (b) The higher field range resolves at least 19 frequencies and enhances the amplitude of frequencies in the intermediate range.

in Fig. 4. The background dc magnetoresistance rises faster than linear at low fields and becomes linear above 70 kG for field directions in the $\hat{a}$-$\hat{c}$ plane perpendicular to the $\hat{b}$ axis.

The ac magnetoresistance results detect a great many frequencies and we have been able to track most of them over a reasonable angular range. Typical transverse ac magnetoresistance curves are shown in Fig. 9 for two different field ranges. The Fourier transforms corresponding to these field sweeps are shown in Fig. 10. Both transforms show a large number of frequencies in the range 0.7–21 MG. In the case of $TaSe_3$ the high field sweeps with large-amplitude modulation show additional frequencies as well as reproducing those observed at lower fields. This suggests that many small Fermi-surface sections exist in $TaSe_3$ and that the distribution of cross sections, effective masses, and $\omega_c\tau$ values are in the range for excellent detection by the field ranges and modulations available in the present experiments. This contrasts with $NbSe_3$ where the data at high fields do not detect frequencies other than those already present at the intermediate fields.

For fields in the plane perpendicular to $\hat{b}$ most of the frequency branches show a minimum at the same angle and rise rapidly on either side of this minimum, as shown in Fig. 11. Data corresponding to harmonics have not been plotted in Fig. 11. The solid lines drawn for these branches in Fig. 11 represent functions of the form $\omega_0/\cos\theta$. All of these frequencies track out to angles in the range 30°–60° from the minimum. At greater angles than shown in Fig. 11 the amplitudes decrease rapidly and cannot be accurately tracked. The two lowest frequencies do not exhibit the same orientational symmetry as the upper branches and they also show considerably less anisotropy. This behavior is not inconsistent with the monoclinic crystal structure, where the $\hat{a}$ and $\hat{c}$ axes lie at angles of ~106°.

A limited amount of angular data has also been obtained for field angles rotated out of the $\hat{a}$-$\hat{c}$ plane toward the $\hat{b}$ axis. Data corresponding to fields in a plane containing the $\hat{b}$ axis and cutting the $\hat{a}$-$\hat{c}$ plane at an angle 14° off the minimum frequency point in the $\hat{a}$-$\hat{c}$ plane are shown in Fig. 12. These frequency branches show a minimum in the

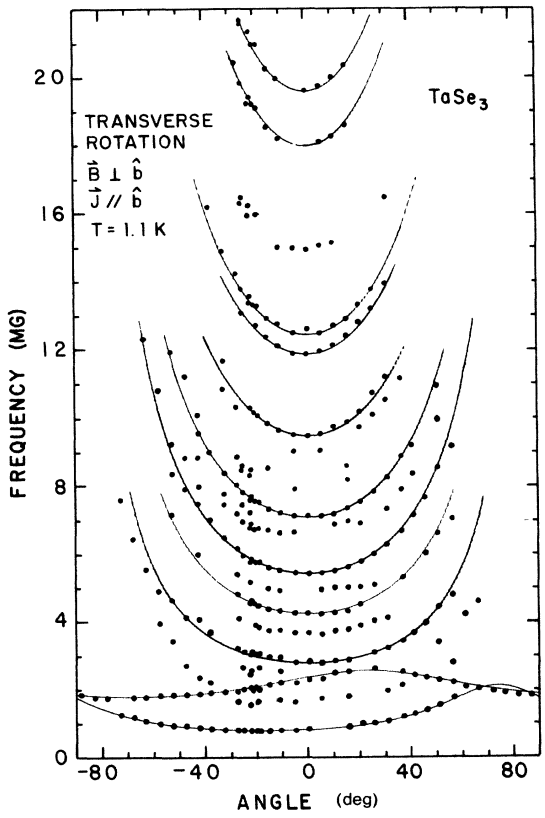

FIG. 11. Angular dependence of the frequencies in $TaSe_3$ observed for field directions lying in the $\hat{a}$-$\hat{c}$ plane. Values of the frequencies at the minimum are also listed in Table I.

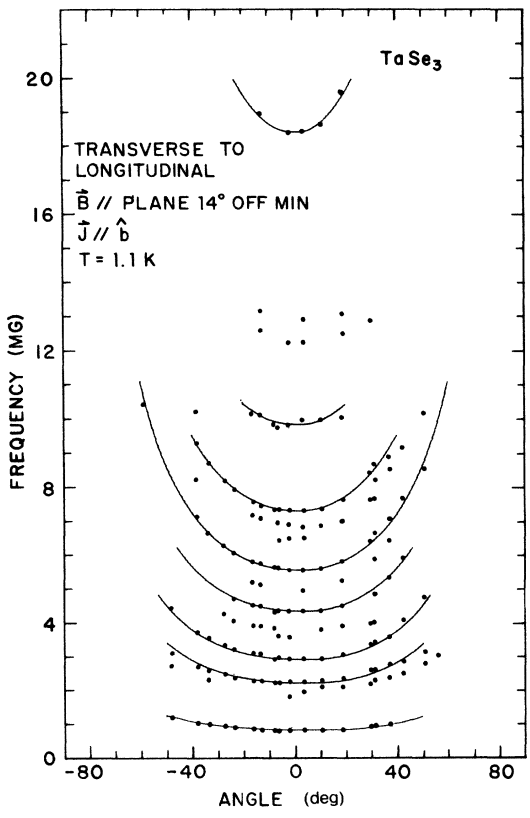

FIG. 12. Angular dependence of the frequencies in $TaSe_3$ observed for field directions rotated from the $\hat{a}$-$\hat{c}$ plane toward the $\hat{b}$ axis and cutting the $\hat{a}$-$\hat{c}$ plane 14° off the minimum-frequency direction.

$\hat{a}$-$\hat{c}$ plane and increase rapidly as the field is rotated toward the $\hat{b}$ axis. The solid lines again represent the function $\omega_0/\cos\theta$.

C. Hall effect in $NbSe_3$

The Hall effect has been measured in $NbSe_3$ for field perpendicular to the plane of the ribbon and Hall leads in the plane of the ribbon. The Hall resistance in the temperature range from 4.2 to 300 K in a field range from 0 to 150 kG is shown in Figs. 13. As the temperature is decreased through the 59-K phase transition the Hall voltage reaches a positive maximum and then decreases and becomes entirely negative at 4.2 K. At intermediate temperatures between 4.2 and 40 K, there is a strong nonlinear field dependence which drives the Hall voltage through a positive maximum, and then negative at higher fields. This anomalous behavior is observed only below the 59-K transition, while no unusual behavior is observed as the temperature passes through the 145-K transition.

IV. DISCUSSION

The frequencies detected in the oscillatory magnetoresistance of $NbSe_3$ demonstrate the existence of several small pieces of Fermi surface representing 10^{-3}–10^{-2} of the cross-sectional area of the Brillouin zone. Three or four frequencies in the range 0.28–3 MG have been detected in $NbSe_3$, while the area of the Brillouin zone perpendicular to $\hat{c}$ corresponds to a frequency of ~125 MG. In $TaSe_3$ at least 20 frequencies in the range 0.7–22 MG have been detected with the highest frequencies representing ~20% of the zone. Although the low-frequency sections are of comparable magnitude in both metals, higher-frequency branches are only observed in $TaSe_3$. Since the $NbSe_3$ crystals

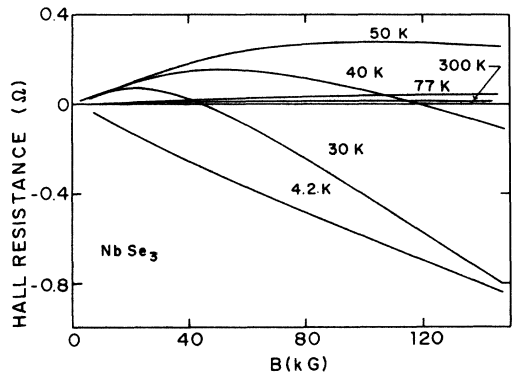

FIG. 13. Hall resistance in $NbSe_3$ measured in the temperature range 4.2–300 K for field perpendicular to the plane of the ribbon and in a range 0–150 kG. A rapid decrease and change of sign occurs below the 59-K transition.

exhibit larger residual-resistance ratios than $TaSe_3$, the observation of higher frequencies in $TaSe_3$ suggests that a significant difference exists between the two Fermi surfaces. This difference can simply be due to the absence of larger sections in $NbSe_3$ or it is also possible that sections exist with effective masses or areas too large to be detected with the present techniques.

It can be speculated that the phase transitions occurring in $NbSe_3$ produce a major change in Fermi surface. If these are due to the onset of charge-density waves, then the accompanying gapping and superlattice formation can remove a large fraction of the Fermi-surface area. On the basis of the increase in resistivity Ong and Monceau[2] estimate that a loss in Fermi-surface area of 20% occurs at the 145-K transition and that 62% of the remaining Fermi surface is destroyed by gaps at the 59-K transition. This would produce the large increase in resistivity observed at the phase transitions in $NbSe_3$ and the loss of cross-sectional areas corresponding to the higher frequencies similar to those observed in $TaSe_3$. However, a decrease of mobility and change in effective mass at the transitions could also increase the resistance and reduce the observability of larger Fermi-surface sections.

If the resistance transitions in $NbSe_3$ are due to CDW formation, then they would be more comparable to those observed in the 1*T* phase of layer structure dichalcogenides with octahedral coordination. These show large resistance increases below the CDW transition in contrast to the 2*H* phase trigonal coordination layer structures which generally become better metals below the transition. In fact, Fleming and Coleman[9] have shown that in the CDW phases of the trigonally coordinated layer dichalcogenides 2*H*-$TaSe_2$ and 4*Hb*-TaS_2 the oscillatory magnetoresistance indicates that the CDW superlattice produces many additional small sections of Fermi surface corresponding to a range of frequencies similar in magnitude to those observed in $TaSe_3$. No definite conclusions about CDW's in $NbSe_3$ can be established at present other than to point out the clear experimental difference in the number and cross-sectional areas of the Fermi-surface sections observed in $NbSe_3$ and $TaSe_3$.

The angular dependence of the frequencies observed in both $NbSe_3$ and $TaSe_3$ show substantial anisotropy as would be expected from the crystal structure. Data on the angular dependence are complete enough to conclude that the Fermi surfaces are three dimensional and generally consistent with elongated flattened ellipsoids, although a precise determination of the anisotropies of all sections has not been made. The details and

extent of the present analysis for the two materials are given below.

A. $NbSe_3$

For field rotations in planes both perpendicular and parallel to $\hat{b}$, the main Fermi-surface section contributing to the quantum oscillations shows strong anisotropy. The minimum frequency of 0.28 MG occurs for $\vec{B}$ perpendicular to the $\hat{b}$ axis (whisker axis) and in the plane of the ribbon. For rotation in the plane perpendicular to $\hat{b}$ the maximum observed anisotropy of the upper-frequency branch is approximately 3.4, while the lower branch can be fitted with an anisotropy of 1.4. For rotation out of the $\hat{a}$-$\hat{c}$ plane toward the $\hat{b}$ axis the anisotropy is larger with an anisotropy ratio of at least 8. This behavior would be consistent with a pancake-shaped section of Fermi surface lying in the plane perpendicular to $\hat{b}$ and having an elliptical cross section in this plane with the thin dimension of the pancake along $\hat{b}$.

The above model is consistent with the metal-atom spacing of the lattice which would give the highest conductivity along $\hat{b}$ and low conductivity in the $\hat{a}$-$\hat{c}$ plane, but with considerable anisotropy in the $\hat{a}$-$\hat{c}$ plane. This low-frequency section and its harmonics completely dominate the quantum oscillations observed in both the dc and ac magnetoresistance. The anisotropies measured for this section should be considered as lower limits, since the data at high angles show progressively weaker amplitudes and are not accurate enough at the critical high angles to set a precise upper limit on the anisotropy.

The lowest frequency is the only frequency observed in the dc data, but the more sensitive ac results show a number of low-amplitude Fourier components corresponding to frequencies up to 5.2 MG. We have not been able to consistently track any of these over a sufficient angular range to obtain information on their shape. We therefore conclude that although one Fourier component dominates the oscillatory behavior, additional Fermi-surface sections are present in $NbSe_3$.

The temperature dependence of the amplitude for the strong low-frequency component has also been measured for $\vec{B}$ transverse to $\hat{b}$ and in the plane of the ribbon. The amplitude of the magnetoresistance oscillation $\Delta\rho/\rho_{sc}$ has been measured at a constant field in the temperature range 1.1–4.2 K, where ρ_{sc} is the semiclassical background magnetoresistance. The resulting normalized amplitudes are then fit by computer to a function of the form $X/\sinh(X)$, which represents the expected temperature dependence of the oscillations.[10] In this function $X = 2^2 m^* k_B T/e\hbar B$ and m^* is adjusted for the best fit. The resulting fit for

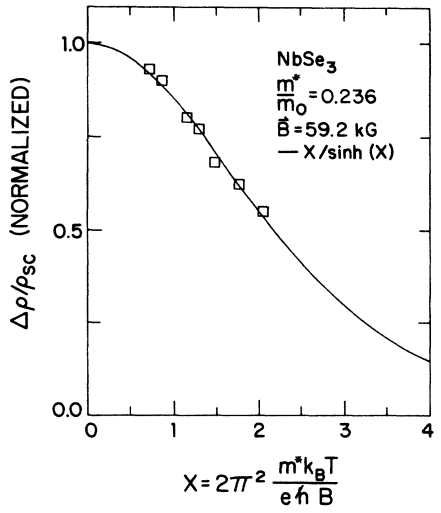

FIG. 14. Temperature dependence of the amplitude of the oscillatory magnetoresistance for the lowest-frequency component in $NbSe_3$ in the range 1.1–4.2 K. The solid curve represents the function $X/\sinh(X)$, where $X = 2\pi^2 m^* k_B T/e\hbar B$. The value of the effective mass determined from this fit is $m^*/m_0 = 0.236$.

$\vec{B}$ = 59.2 kG is shown in Fig. 14 and gives a value of $m^*/m_0 = 0.236$, where m_0 is the free-electron mass. This is a relatively heavy mass for such a small section of Fermi surface and indicates that $NbSe_3$ may have rather flat bands with less mobile electrons below the phase transitions.

The low frequency develops a strong second harmonic at higher fields as shown in the dc magnetoresistance curve of Fig. 4. The presence of higher harmonics may be enhanced by spin splitting of the Landau levels in the magnetic field. The value of the spectroscopic g factor associated with this spin splitting has been estimated by fitting the dc oscillatory magnetoresistance to the following expression[10] for the sum over harmonics of order r.

$$\left(\frac{\Delta\rho}{\rho_{sc}}\right) = A\,\frac{5}{2}\sum_r \left(\frac{B}{F}\right)^{1/2} \beta_r \frac{(-1)^r}{(2r)^{1/2}} \times \cos(\pi v r)\cos\left(\frac{2\pi F}{B} + \phi\right), \quad (1)$$

where A is a constant scale factor and F is the frequency. The term $\cos(\pi v r)$ mixes higher harmonics due to spin splitting with $v = (gm^*/2m_0)$. β_r includes both collision and thermal broadening and is given by

$$\beta_r = \frac{X_r}{\sinh X_r} \exp\left(\frac{-r 2\pi^2 m^* k_B T_D}{e\hbar B}\right), \quad (2)$$

where T_D is the Dingle temperature. Using the value of 0.236 for the effective mass as determined

in Fig. 14, the best fit to the data is obtained with a Dingle temperature $T_D = 2.3$ K and $g = 3.2$ which is the lowest allowed value in the series $g = 3.2 + 4nm_0/m^*$, (n = integer). Measurement of the harmonic content as a function of temperature could be used to further limit the possible g values.[11] The fit to the data is shown in Fig. 15 and includes only second harmonic. If the third harmonic is included in the sum the fit is even better as would be expected, since the ac Fourier transforms show the third harmonic to be present as well.

An additional point which should be considered concerns the magnitude of the measuring current. Monceau *et al.*[1] showed that the non-Ohmic behavior observed below the resistive transitions was also associated with a depression of the transitions at high-current densities. We have used measuring currents in the range 1–30 MA for the magnetoresistance measurements corresponding to current densities in the range 1–30 A/mm^2 and have not observed any current dependence of the frequency components. The transition at 145 K is progressively depressed for current densities in the range 18–140 A/mm^2 but not fully removed.[1] The transition at 59 K is progressively depressed in the range 1–100 A/mm^2 and is almost completely gone[1] for current densities above 100 A/mm^2. Our measurements are carried out at the lower end of these current-density ranges and we therefore expect only a small depression of the resistive transitions. We have measured the transitions in our crystals and find them comparable to those observed by Monceau *et al.*[1]

B. $TaSe_3$

The $TaSe_3$ data show many frequency branches with the two lowest-frequency branches showing little anisotropy. At large-field angles, as measured from the frequency-branch minima, the amplitudes of the higher frequencies decrease rapidly so that precise anisotropies are not determined. As shown by the solid lines in Figs. 11 and 12, functions of the form $\omega_0/\cos\theta$ fit the data quite well. This indicates a fairly large anisotropy, but only defines an approximate minimum anisotropy between 5 and 10 for the 5.7-MG frequency and smaller anisotropies for the higher frequencies. A similar angular dependence for field directions in planes of measurement both perpendicular and parallel to $\hat{b}$ is observed for all but the two lowest frequencies. The most likely forms for these Fermi-surface sections are therefore elongated ellipsoids with the major axes perpendicular to $\hat{b}$. The rapid decrease of amplitude at higher-field angles is also consistent with a fairly rapid increase in the area and effective mass of the extremal orbit and a corresponding reduction in the Shubnikov–de Haas amplitude. Either higher fields or higher-quality crystals will be needed to track these brances to sufficient angles for a precise determination of the anisotropy. The two lowest-frequency branches would be consistent with pancake-shaped sections similar to that proposed for the lowest branch of $NbSe_3$. The estimated anisotropies for these branches assuming an ellipsoidal model are 1.45 and 2.70. The frequencies and cross-sectional areas corresponding to the minima for all branches are listed in Table I.

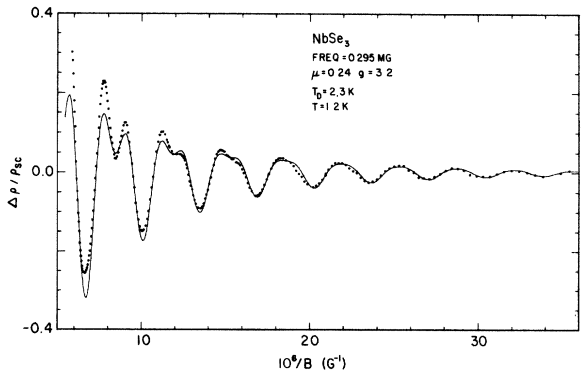

FIG. 15. The oscillatory component of the dc magnetoresistance as shown in Fig. 4 plotted as the dotted curve. Solid curve represents the function given in Eq. (1) with parameters $\mu = m^*/m_0 = 0.24$, $g = 3.2$, $T_D = 2.3$ K, and $F = 0.295$ MG.

TABLE I. Minimum Fermi-surface [a] cross sections in $TaSe_3$.

	Frequency (MG)	Area (10^{-2} Å^{-2})
1	0.8	0.77
2	1.8	1.7
3	1.7	1.6
4	2.8	2.7
5	3.7	3.5
6	4.3	4.1
7	4.9	4.7
8	5.4	5.2
9	6.7	6.4
10	7.1	6.8
11	9.0	8.6
12	9.5	9.1
13	10.8	10.3
14	11.9	11.4
15	12.6	12.1
16	14.4	13.8
17	15.0	14.4
18	16.3	15.6
19	18.0	17.2
20	19.6	18.8

[a] Cross section of Brillouin zone corresponds to ~125 MG.

V. CONCLUSIONS

The magnetoquantum oscillations observed in $NbSe_3$ and $TaSe_3$ show a distinct difference in the number of Fermi-surface sections that can be detected. Both metals show low frequencies in the range 0.1–1 MG, but only $TaSe_3$ shows many equally strong frequencies in a continuous range up to 22 MG. In $NbSe_3$ a low-frequency branch with a minimum frequency of 0.28 MG, and a giant amplitude completely dominates the quantum oscillatory behavior over the entire field range for fields near the plane of the ribbon. An analysis of the data on the temperature dependence of the amplitude gives a value of $0.24m_0$ for the effective mass of this orbit. In addition, a fit to model expressions including a harmonic mixing term resulting from spin splitting of the Landau levels gives a minimum g value of 3.2 and a Dingle temperature of 2.3 K. The Fourier transforms indicate the existence of weak higher frequencies in the range 1–5 MG, but these are too weak to track adequately.

Of the 20 or so frequencies observed in $TaSe_3$, six or more show strong amplitudes and the remainder show a distribution of weaker amplitudes. The high-field sweeps bring up the amplitudes of additional frequencies as compared to the low-field sweeps and indicate a wide distribution of effective masses and cross sections with characteristic parameters for excellent detection in the present experiments.

The lowest-frequency section in both $NbSe_3$ and $TaSe_3$ show relatively low anisotropy in the $\hat{a}$-$\hat{c}$ plane in the range 1.4–3.4, while the anisotropy from the $\hat{a}$-$\hat{c}$ plane to the $\hat{b}$ axis shows a minimum value of ~8. The higher frequencies in $TaSe_3$ show an anisotropy of at least 5–10 in both the $\hat{a}$-$\hat{c}$ plane and toward the $\hat{b}$ axis, although the rapid decrease of the amplitudes at high-field angles relative to the minimum-frequency direction make the precise anisotropy undetermined. The general behavior is consistent with elongated elipsoidal surfaces with the major axes of the ellipsoids perpendicular to the $\hat{b}$ axis.

The existence of only one dominant amplitude at low frequency in $NbSe_3$ as compared to the large number of equally strong frequencies in $TaSe_3$ may possibly be connected with the existence of the two resistive transitions in $NbSe_3$, which are not observed in $TaSe_3$. If these are associated with CDW transitions, then the gapping associated with the CDW can remove fairly large sections of Fermi surface. Preliminary measurements of the Hall effect show the onset of a rapid change below the 59-K transition and a change in sign from positive to negative at the lowest temperatures. This suggests a substantial change in band structure or mobility over an extended range of temperature below the transition. This is not inconsistent with a large change in Fermi surface through the transition. The precise nature of the transitions in $NbSe_3$ and the source of the differences in the Fermi-surface sections of $NbSe_3$ and $TaSe_3$ will require further investigation, but the present results give a good basis for further consideration.

ACKNOWLEDGMENTS

The authors would like to thank Estelle Phillips for many contributions to the crystal growth program and Larry Rubin for valuable help with the instrumentation at the National Magnet Laboratory. Dr. William Lowrey provided valuable assistance for the run at the Naval Research Laboratory.

---

*Work above 80 kOe was performed while the authors were Guest Scientists at the Francis Bitter National Magnet Laboratory, which is supported at the Massachusetts Institute of Technology by the NSF. Work above 80 kOe was also performed at the Naval Research Laboratory.

†Work supported by the U. S. ERDA Contract No. EY-76-5-05-3105.

[1]P. Monceau, N. P. Ong, A. M. Portis, A. Meerschant, and J. Rouxel, Phys. Rev. Lett. 37, 602 (1976).

[2]N. P. Ong and Pierre Monceau (unpublished).

[3]J. A. Wilson, F. J. DiSalvo, and S. Mahajan, Adv. Phys. 24, 117 (1975).

[4]A. Meerschant and J. Rouxel, J. Less-Common Metals 39, 197 (1975).

[5]E. Bjerkelund, J. H. Fermor, and A. Kjehshus, Acta Chem. Scand. 20, 1836 (1966).

[6]P. Monceau, J. Peyrand, J. Richard, and P. Molinie, Phys. Rev. Lett. 39, 160 (1977).

[7]Takanshi Sambongi, Masafumi Yamamoto, Kitomi Tsutsumi, Yoichi Shiozaki, Kayuhiko Yamaya, and Yutaka Abe, J. Phys. Soc. Jpn. Lett. 42, 1421 (1977).

[8]R. W. Stark and L. R. Windmiller, Cryogenics 8, 272 (1968).

[9]R. M. Fleming and R. V. Coleman, Phys. Rev. B 16, 302 (1977).

[10]Laura M. Roth and Petros N. Argyres, in *Semiconductors and Semimetals*, edited by R. K. Willardson and Albert C. Beer (Academic, New York, 1966), p. 159.

[11]A. V. Gold and P. W. Schmor, Can. J. Phys. 54, 2445 (1976).